Experimental study of entropy generation during condensation in inclined enhanced tubes

Adelaja, A.O.[1,2*], Dirker, J.[1], Meyer, J.P.[1***]**

[1]Department of Mechanical and Aeronautical Engineering, University of Pretoria, Pretoria, 0002, South Africa

[2]Department of Mechanical Engineering, University of Lagos, Akoka, Yaba, Lagos, 101017, Nigeria

**Corresponding Author:*

E-mail: aadelaja@unilag.edu.ng

Phone: +234 806 812 3861

***Alternative corresponding author:*

E-mail: jaco.dirker@up.ac.za

Phone: +27 12 420 2465

****Alternative corresponding author:*

E-mail: josua.meyer@up.ac.za

Phone: +27 12 420 3104

Abstract

In the current study, the influence of inclination angle, temperature difference, mass velocity, and vapour quality is investigated on the entropy generation rate in an inclined enhanced tube during the flow condensation of R134a. The enhanced tube is a microfinned tube with a helix angle of 14°. The experiments are carried out at a saturation temperature of 40 °C, heat fluxes of 230–270 W, mass velocities between 200 and 400 $kgm^{-2}s^{-1}$, qualities of 10–90%, and inclination angles between -90° and +90°. Results show that the frictional contribution becomes significant when compared with the heat transfer component of the total entropy generation rate at the mass velocities ≥300 $kgm^{-2}s^{-1}$. The overall minimum total entropy generation corresponds to the mass velocity of 300 $kgm^{-2}s^{-1}$, quality of 25%, and inclination angle of +5°, while the maximum total entropy generation is obtained for the mass velocity of 400 $kgm^{-2}s^{-1}$, inclination angle of -60°, and quality of 90%. For optimal design, the inclination angle of $-10^\circ \leq \beta \leq +10^\circ$ is proposed for minimal total entropy generation for vapour qualities less than 75%, and $+90^\circ$ for qualities greater.

Keywords: Inclination angle; condensation; entropy generation rate; heat transfer coefficient; pressure drop; enhanced tube

Nomenclature

c_w	Water specific heat, $J\ kg^{-1}K^{-1}$
d	Diameter, m
g	Gravitational acceleration, ms^{-2}
G	Mass velocity, $kgm^{-2}s^{-1}$
h_{fg}	Latent heat, $J\ kg^{-1}$
L	Length, m
$\dot{m}$	Mass flow rate, kgs^{-1}
Q	Heat transfer rate, W
$\dot{S}$	Entropy generation rate, WK^{-1}
T	Temperature, °C
x	Quality

Greek words

β	Inclination angle, ○

ε	Void fraction
ρ	Density, kgm^{-3}

Subscript	
Δp	Pressure difference
fric	Friction
gen	Generation
h	Heat transfer
in	Entrance
l	Liquid
m	Mean
opt	Optimal
out	Exit
Q	Heat transfer
ref	Refrigerant
sat	Saturation
test	Test section
T	Total
tp	Two-phase
v	Vapour
w,i	Wall
w	Water

1.0 Introduction

The importance of heat exchange equipment cannot be over-emphasised due to its applications in major industrial sectors such as power plants (thermal and nuclear), refrigeration, heating ventilation, and air conditioning (HVAC) plants, and chemical and processing plants. Although most heat exchangers are horizontally installed, inclined tubes are used in air-cooled condensers in air conditioning and refrigeration systems, power plants, etc.

A quantitative analysis of the quality of the design performance of heat exchange equipment is necessary for the estimation of energy transformation in energy systems. Entropy

generation is an estimation of the degree of irreversibility in a system. It is utilised to evaluate the quality of the transformation of thermal energy. The major source of irreversibility has been related to heat transfer and fluid frictional pressure drop.

Improving the efficiency of energy systems is very critical today due to scarce resources and concerns about climate change. Minimising entropy, however, is crucial to the effective and efficient design of these systems. McClintock (1951) was the first to apply entropy generation minimisation to analyse heat exchange systems. Other authors have since used the method to evaluate complex systems (Bejan, 1977, 1978, 1980; Bejan et al., 1995; Kaiser, 1993; Ranasinghe and Reistad, 1990). Entropy generation results in the destruction of the available energy, reducing the efficiency of the system. It is, therefore, necessary to minimise the entropy generation rate attributable to the prevailing phenomena in the heat exchange system, such as boiling, evaporation, and condensation.

A few papers on the subject of entropy generation will be reviewed here. Bejan (1979, 1996, 2000) presented the fundamentals of entropy generation minimisation and applied them to the examination of single-phase-flow heat transfer in engineering equipment. Lin et al. (2001), in their study of the second law of thermodynamics in a condensing unit in horizontal orientation conveying R22, noted that minimum entropy generation was achieved at an optimal temperature and was dependent on mass flow rate and tube geometry. Cavallini (2002) employed the penalty factor approach to analyse a condensing unit conveying a two-phase flow refrigerant. The total entropy generation attributed to the heat transfer and frictional pressure drop was considered during the optimisation to obtain the optimal condensing length. Galovic et al. (2003) studied entropy generation in parallel, countercurrent, and cross-flow heat exchange systems with respect to temperature variation, and defined related entropy generation as the ratio of the actual to maximum entropy generation. Adeyinka and Naterer (2004) investigated entropy generation in a flat plate and developed a correlation for the optimisation of laminar film condensation. Saouli and Aïboud-Saouli (2004) applied the second law of thermodynamics to analyse falling film in inclined heated plates during laminar flow condensation. They observed that irreversibilities due to fluid friction were significantly larger than those ascribable to convective heat transfer. Therefore, it was the controlling parameter.

Li and Yang (2006), in a study on the elliptic cylinder in horizontal orientation, found that surface tension was significant when the ellipticity was greater than 0.7. Yang et al. (2007)

considered the same physical model in their study, but this time imposed variable wall temperature. It was noted that the amplitude of the variable wall temperature was proportional to the entropy generation. Chen et al. (2008) considered a circular tube in horizontal orientation for the study of entropy generation minimisation during convective film condensation. They concluded that the reduction of the Brinkman parameter would minimise entropy generation. Sahiti et al. (2008), in their study of entropy generation reduction in various pipe-in-pipe heat exchange equipment conveying air and water, found that flow length and various circumferential pin fins were optimised. They noted that the Reynolds number was a function of entropy generation. Their result was in agreement with the conclusions of Ratts and Raut (2004) in their work on single-phase flow. They also reported the dependence of entropy generation rate on the Reynolds number. Saechan and Wongwises (2008) employed the entropy generation minimisation of refrigerant and air to evaluate the optimum system configuration of a plate-type air-refrigerant condensing unit. The entropy generation was employed to optimise the arrangement. They concluded that the greater part of the entropy generation was contributed by the airside. Revellin et al. (2009) thermodynamically analysed the two-phase flow of pure fluids in smooth and enhanced tubes, using the separated flow and mixture models. From the proposed model, especially the mixture model, it was noted that enhanced tubes were recommended for lower mass velocities (<235 $kgm^{-2}s^{-1}$), while smooth tubes were better for higher mass velocities as they exhibited reduced entropy generation accordingly. Gheorghian et al. (2015) evaluated 30 heat transfer contact surfaces comprising plain, louvered, and strip fins, and suggested an entropy generation standard for evaluating the surfaces of compact heat exchange systems for different mass flow rates and fluid temperatures. Wang and Huai (2018) experimentally studied the convective heat transfer and entropy generation of a lithium bromide exchanger (LBE): a helium two-loop heat exchange system. In the study, the effects of effectiveness, number of transfer unit (NTU), pumping power, Reynolds number, mass flow rate, and inlet temperature on the entropy generation were investigated. It was noted that entropy generation increased as inlet temperature, mass flow rate, LBE inlet temperature and pumping power increased. The effects of NTU and the effectiveness and ratio of the heat capacities were insignificant. Wang et al. (2018) investigated the effects of corrugation height and pitch on flow distribution and entropy generation resulting from the convective heat transfer, and frictional pressure drops around the wall region. They showed that the effect of the contribution of friction was only significant at the windward side of the corrugation

and was influenced by gradients inflow velocity. The heat transfer contribution could nevertheless be enhanced by secondary flow, produced by the effect of corrugation. They concluded that optimal entropy generation occurred when the Reynolds number was less than 30500.

Imteyaz and Zubair (2018) numerically studied the influence of pressure drop and axial conduction on thermal performance and exergy loss in a microfin double tube heat exchanger. It was noted that, for a low viscous fluid, fluid frictional irreversibility was negligible at low mass flow rates. At a high mass flow rate, frictional entropy generation was also higher than heat transfer entropy generation. Ahmad et al. (2018) experimentally studied the exergy evaluation of a double-tube heat exchanger in a co-current flow arrangement. The hot and cold water flowed through the inner tube and annulus, respectively. The mass flow rate of the hot water was varied between 0.016 and 0.479 kgs^{-1} and that of the cold water between 0.0326 and 0.572 kgs^{-1}. The mass flow rate was investigated for effectiveness, entropy generation rate, and exergy loss. Khaboshan and Nazif (2019) numerically studied the convective heat transfer and entropy generation of an alternating elliptical axial (AEA) tube with different pitch angles at a constant wall temperature. It was observed that the increase in pitch angle and Reynolds number increased the Nusselt number and friction factor. The total entropy generation also had the greatest contribution from the convective heat transfer component, and the ratio of the minimum entropy generation between the AEA and the circular tube occurred at a Reynolds number of 20000. Zhang et al. (2019) numerically studied the effects of mass velocity, pressure, heat flux, cross-sectional shape, and buoyancy on the thermodynamic performance of a supercritical pressure CO_2 using the second law of thermodynamics. Results showed that the smaller the pressure and ratio of heat to mass velocity, the smaller the entropy generation.

Kumar and Ilangkumaran (2019) experimentally studied the thermal performance and exergy evaluation of an internally grooved tube with a triangular cut twisted tape (TCTT) insert with a ratio of 3.5, 5.3, and 6.5, and an angle of attack of 45^o and 90^o. It was noted that the thermal and exergy efficiencies of the TCTT's internally grooved tube increased by 12 and 85%, respectively, when compared with the plain twisted tape. Chen et al. (2019) provided a comprehensive review of two theories – entropy and entransy – based on optimisation criteria, methods, and results. The merits and demerits of the theories were evaluated. However, the authors noted that entropy generation might not be applicable to all practical systems for the evaluation of minimum entropy generation, which they claimed might not coincide with maximum heat transfer.

Holagh et al. (2020) investigated the impact of twist pitch, mass velocity, tube diameter, saturation temperature, and vapour quality on entropy generation during convective boiling in heat exchangers with twisted tape inserts. They noted that tubes with larger diameters and higher qualities had higher entropy generation, while increased twisted pitch and saturation temperature reduced entropy generation. The effects of mass velocity showed an initial decrease to a minimum before a gradual increase in entropy generation. See and Leong (2020), in their numerical study of entropy generation during flow boiling in a semi-circular mini-channel, considered the influence of heat flux, mass velocity, channel diameter, and inlet pressure. The effect of mass velocity was only significant in channels with a small diameter. Channels with a large diameter produced higher total entropy generation and the contribution of convective heat transfer to the total entropy generation when compared with the frictional pressure contribution. Finally, increasing the inlet pressure drop decreased entropy generation. Keklikcioglu et al. (2020) experimentally studied entropy generation in a heat exchanger with wire inserts of diverging, converging conical and converging-diverging configurations when ethylene glycol and water mixtures were made to flow in the system. Results showed that a configuration of converging conical wire inserts gave the highest entropy generation rate of the three, while the diverging configuration gave the lowest entropy generation rate. The value of 0.42 was the lowest entropy generation attained. It was obtained with pure water and a diverging conical configuration of pitch ratio of 2 at Reynolds number 6882. Abu-Hamdeh et al. (2020) numerically investigated energy and exergy loss in a finned tube heat exchanger. Results indicated that optimal exergy loss was obtained when the Reynolds number was 8333, with a Prandtl number of 10.63 and a transverse pitch of 3.52. Zhao et al. (2020) applied the theory of the field synergy principle to the improvement of the thermal capacity of a finned heat exchanger by 7%. With the proposed principle applied to enhance heat transfer, the total entropy generation rate was improved.

From the literature studies reviewed, experimental investigations of entropy generation in inclined enhanced heat exchangers, which involve the whole range of inclination angles, are found to be rare. Most of the studies are limited to horizontal and vertical tube orientations due to their applications; however, in industrial A- and V-frame heat exchangers, the tube orientations are inclined. Also, for the installation of heat exchangers in situations where there are space constraints, during automobile navigation uphill and downhill and aeroplane takeoff, landing, and banking. During two-phase flow in inclined heat exchangers, the flow patterns are altered due to gravitational

pull, but this effect on entropy generation rate is yet to be understood. Therefore, this study focuses on the influence of inclination angle, vapour quality, mass velocity, and temperature difference on the contributions of convective heat transfer and pressure drop to total entropy generation rate, total entropy rate, and Bejan number in an inclined, enhanced condensing unit. This may be informative and useful for heat exchange design and optimisation.

2.0 Experimental Procedure

Fig. 1 shows a sketch of the study test bench employed in this study. It was a vapour compression system driven by a scroll compressor through which vapour refrigerant was pumped into two high-pressure lines. One of the lines housed the pre-, test- and post-condensing units with an electronic expansion valve (EEV). The second line accommodated the bypass condensing unit with another electronic expansion valve. The bypass unit regulated the quantity of refrigerant that flowed through the first high-pressure line. These two lines meet to discharge the liquid refrigerant into the low-pressure line, which houses the evaporating unit and suction accumulator. The cycle was completed as dry vapour exited the accumulator and entered the compressor. Each of the heat exchange units, i.e., the condensing and the evaporating units, is connected to a heat pump through which hot water passed into the evaporating unit and cold water passed into the condensing unit. All the equipment used was calibrated using standard procedures. Different thermocouples (T-type with $\pm 0.1^{o}$C accuracy) and pressure transducers (absolute pressure of ± 12 kPa and differential pressure of ± 0.05 kPa accuracies) were connected to different components and sections of the system to measure the temperatures of the refrigerant, cold and hot water, and pressure at different points. Flow meters (of ± 0.1 to ± 0.35% accuracy) were also installed to determine the refrigerant and water flow rates. For example, the thermocouples were calibrated against a high-precision Pt-100 resistance temperature detector to an accuracy of 0.1 °C. The dependability of the reading was checked by comparing the saturation temperature obtained with the absolute pressure transducers and that acquired from the thermocouples. A difference of less than 0.1 °C was obtained at high mass fluxes (> 400 $kgm^{-2}s^{-1}$), while a slightly higher value was noted at lower mass fluxes. This variation could be attributed to the irregular flow patterns encountered for lower mass velocities, i.e. the stratified-wavy, smooth-stratified, and intermittent flow regime.

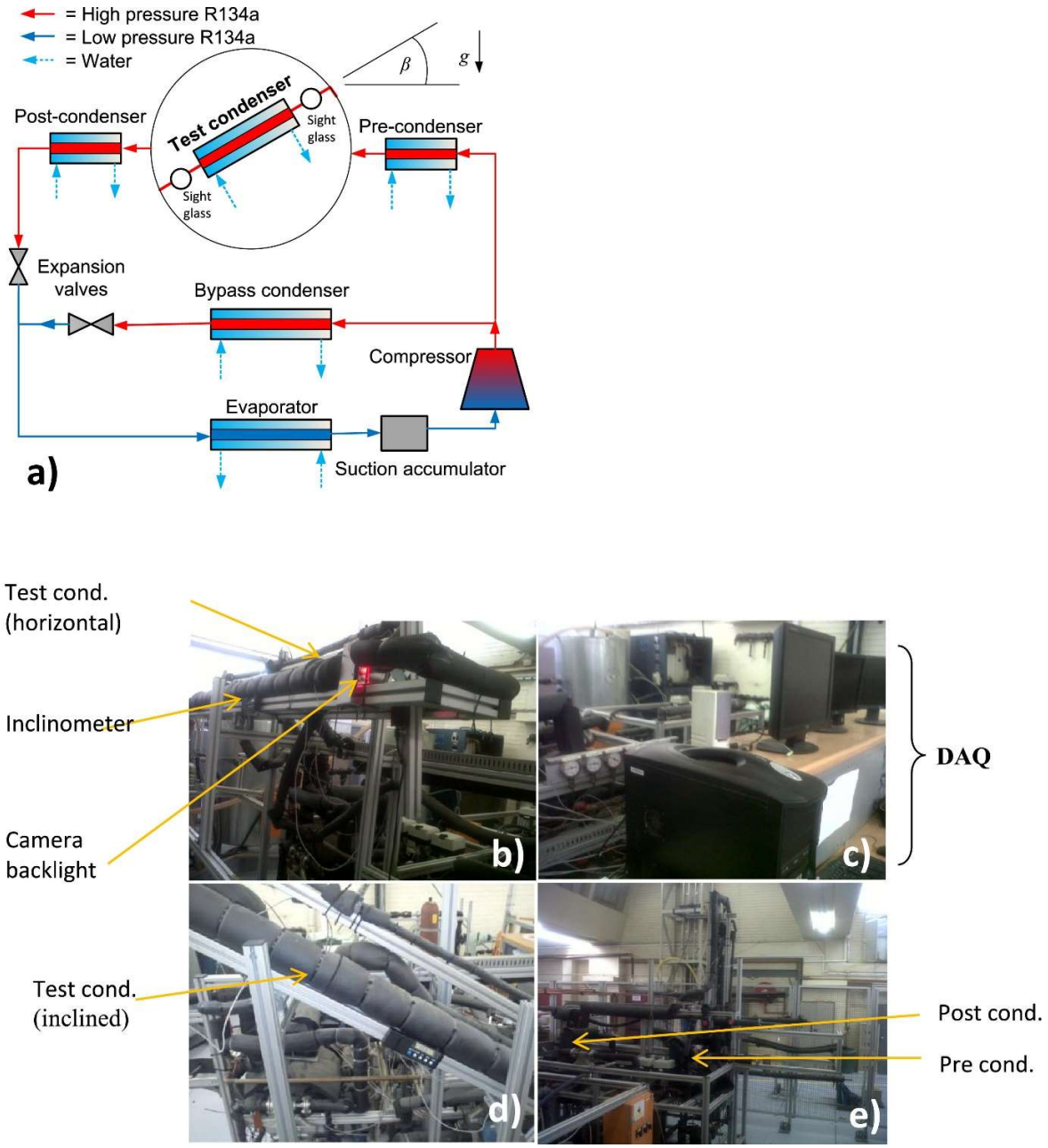

Fig. 1: a) The sketch of the test experimental setup, physical representation of b) the test condenser in horizontal position c) data acquisition (DAQ) system, d) test condenser in inclined angle and, e) pre cond. (pre-condenser), post cond. (post condenser) and some other equipment

The test section, as shown in Fig. 2, had a convective heat transfer length, L_h, of 1.488 m and a differential pressure length, $L_{\Delta p}$, of 1.704 m. It was a tube-in-tube counterflow condensing unit manufactured from hard-drawn thin copper with cold water flowing in the annulus and refrigerant flowing in the inner grooved tube. The inner tube had a mean diameter, d_m, of 8.71 mm, an outer

diameter d_o of 9.55 mm, and an annulus outer diameter of 15.9 mm. Other details of the tubes can be found in Table 1. The links to the test condensing unit were made of high-pressure flexible tubings. These allowed the test section to revolve around two fixed hinges. A calming section of about 50 diameters in length was located at the entrance of the unit so that fully developed flow can be obtained in the test section (Adelaja et al., 2016, 2017; Adelaja, Dirker, et al., 2019; Adelaja, Ewim, et al., 2019; Adelaja, Ewim, et al., 2020; Ewim et al., 2018; Meyer et al., 2014; Meyer and Ewim, 2018).

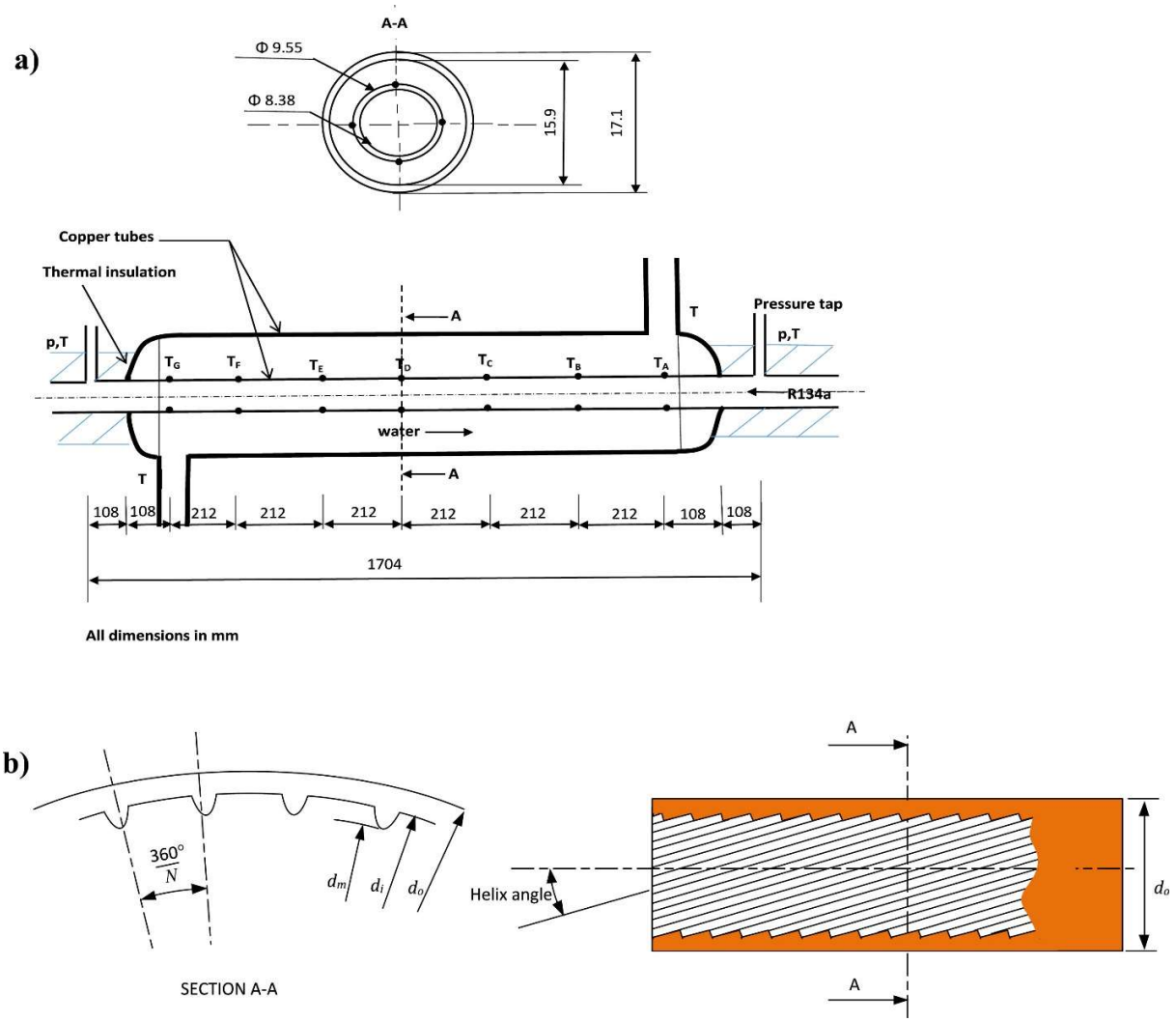

Fig. 2 a) Schematic diagram of the test section with smooth tube, cross-sectional area view and, b) sectional view of the enhanced inner tube

Table 1: Description of the tubes

Description	Value
	Microfin
Inner mean diameter d_m, mm	8.71
Inner diameter d_i, mm	8.92
Outer diameter d_o, mm	9.55
Tube wall thickness, mm	0.32
Fin height e, mm	0.21
Fin pitch, mm	0.445
Circumferential fin number N	60
Helix angle H, [°]	14
Roughness, e/d_i	0.0235

Table 2 presents the data for the test conditions used for the experiment with the maximum variations. The mean vapour quality is the arithmetic mean of the entry, x_{in}, and exit, x_{out}, qualities, respectively. Like all other measurable parameters in the table, data is only collected when the steady-state conditions were attained and the energy balance was less than 3.0%. For each of the more than 120 data points, data was collected through the National Instrument LABVIEW data acquisition system for about two minutes and the average used. This was to ensure that data noise was minimised.

Table 2: Experimental test variables and fluctuations

Parameters	Ranges	Fluctuations
T_{sat}[K]	313.15	±0.6
G [kg/m^{2}s]	200–400	±5.0
x_m [-]	10–90%	±0.01
β [°]	-90° to +90°	± 0.1
Q_{test} [W]	230–270	± 20

3.0 Data Reduction Strategy

The comprehensive information of the data reduction strategy can be located in previous works (Adelaja, Ewim, et al., 2019; Meyer et al., 2014). The entropy generation in the condensing units is due to the combined effect of the convective heat transfer and pressure drop of the two-phase flow

circulating through the test condensing unit (Bejan et al., 1995). The total entropy generation rate is expressed as follows:

$$\dot{S}_{gen,T} = \dot{S}_{gen,Q} + \dot{S}_{gen,\Delta P} \quad (1)$$

Where $\dot{S}_{gen,Q}$ and $\dot{S}_{gen,\Delta P}$ are the entropy generation rates for the convective heat transfer and pressure drop, respectively.

$$\dot{S}_{gen,T} = \dot{Q}\left(\frac{1}{T_{w,i}} - \frac{1}{T_{sat}}\right) + \frac{\dot{m}_{ref}\Delta P_{fric}}{\rho_{tp}T_{sat}} \quad (2a)$$

Eq. (2a) can be written as

$$\dot{S}_{gen,T} = Q\frac{\Delta T}{T_{sat}^2\left(1-\frac{\Delta T}{T_{sat}}\right)} + \frac{\dot{m}_{ref}\Delta P_{fric}}{\rho_{tp}T_{sat}} \quad (2b)$$

Where $\Delta T = T_{sa} - T_{w,i}$ and $\frac{\Delta T}{T_{sat}} \ll 1$

Eq. (2b) after some manipulations can be written as

$$\dot{S}_{gen,T} = \frac{\dot{Q}\Delta T}{T_{sat}^2} + \frac{\dot{m}_{ref}\Delta P_{fric}}{\rho_{tp}T_{sat}} \quad (3)$$

The heat transfer rate is evaluated (Meyer et al., 2014; Adelaja, Dirker, et al., 2019) as

$$\dot{Q} = \dot{m}_w c_w \Delta T_w = \dot{m}_{ref} h_{fg}(x_{in} - x_{out}) \quad (4)$$

Here, h_{fg} is the enthalpy of vaporisation while $\dot{m}_w$, $\dot{m}_{ref}$, c_w, ΔT_w, x_{in}, x_{out}, $T_{w,i}$, T_{sat} and ρ_{tp} are the water and refrigerant mass flow rates, water specific heat capacity, change in water temperature between inlet and outlet, inlet and outlet refrigerant vapour qualities, wall and saturation temperatures, and the two-phase density, respectively.

The frictional pressure drop ΔP_{fric} is determined (Adelaja et al., 2017) as

$$\Delta P_{fric} = \Delta P_{meas} + \Delta P_{line} - \Delta P_{stat} - \Delta P_{mom} \quad (5)$$

where ΔP_{meas}, ΔP_{line}, ΔP_{stat} and ΔP_{mom} are the measured, line, static, and momentum pressure drops. The line pressure is heated between the pressure taps and the transducer. The temperature is kept at about 5–10 °C above the saturation temperature so that only vapour is present. The pressure difference in the measuring lines due to the height difference resulting from different inclination angles ΔP_{line} is determined as

$$\Delta P_{line} = \rho_v g L_{\Delta P} \sin\beta \quad (6)$$

where the vapour density, ρ_v, the gravitational constant, g, is taken as 9.81 ms^{-2}, $L_{\Delta P}$ is the distance (1.704 m) between the two differential pressure taps and β is the inclination angle of the

test section varying between vertical upward (+90°), horizontal (0°) and vertical downward (-90°) tube inclinations. The static pressure drop, ΔP_{stat}, can be evaluated as

$$\Delta P_{stat} = \rho_{tp} g L_{\Delta P} \sin\beta \quad (7)$$

where ρ_{tp} the two-phase density is calculated as

$$\rho_{tp} = \rho_l(1-\varepsilon) + \rho_v\varepsilon \quad (8)$$

Where ρ_l, and ε are the liquid density and the drift flux model of (Bhagwat and Ghajar, 2014), which is suitable for inclined passages.

The momentum pressure drop, ΔP_{mom}, is calculated as

$$\Delta P_{mom} = G^2\left[\left(\frac{(1-x)^2}{\rho_l(1-\varepsilon)} + \frac{x^2}{\rho_v\varepsilon}\right)_{out} - \left(\frac{(1-x)^2}{\rho_l(1-\varepsilon)} + \frac{x^2}{\rho_v\varepsilon}\right)_{in}\right] \quad (9)$$

Where G and x are the mass flux and vapour quality, respectively.

The Bejan number is expressed as

$$Be = \frac{\dot{S}_{gen,Q}}{\dot{S}_{gen,Q}+\dot{S}_{gen,\Delta P}} \quad (10)$$

4.0 Results and Discussion

In this section, the significance of inclination angle, mass velocity, and quality on the temperature difference, total entropy generation rate, convective heat transfer and frictional pressure contributions, and the Bejan number are presented. The quality is varied between 10 and 90%, mass velocity between 200 and 400 $kgm^{-2}s^{-1}$, and inclination between -90° and +90°. In this study, downward, horizontal and upward flows indicate $\beta < 0$, $\beta = 0$ and $\beta > 0$, respectively. An increase in inclination angle implies moving from downward flow to upward flow.

The temperature difference and inclination angle have significantly influenced the flow pattern, hence the heat transfer coefficient (Meyer and Ewim, 2018). The thinner the liquid film at the wall, the smaller the thermal barrier hence the temperature difference. The effect of inclination angle on the heat transfer coefficient and frictional pressure drop has been adequately addressed (Meyer et al., 2014; Adelaja, Dirker, et al., 2019), so it will not be discussed in this paper. Fig. 3 shows the pattern of the difference in temperature between the saturated condensing refrigerant and the inner wall with quality and inclination angle for the mass velocity of 200 $kgm^{-2}s^{-1}$ (Fig. 3a), 300 $kgm^{-2}s^{-1}$ (Fig. 3b), and 400 $kgm^{-2}s^{-1}$ (Fig. 3c). From Eq. (2), the entropy generation due

to heat transfer is directly proportional to the temperature difference, and results indicate that the downward flow is

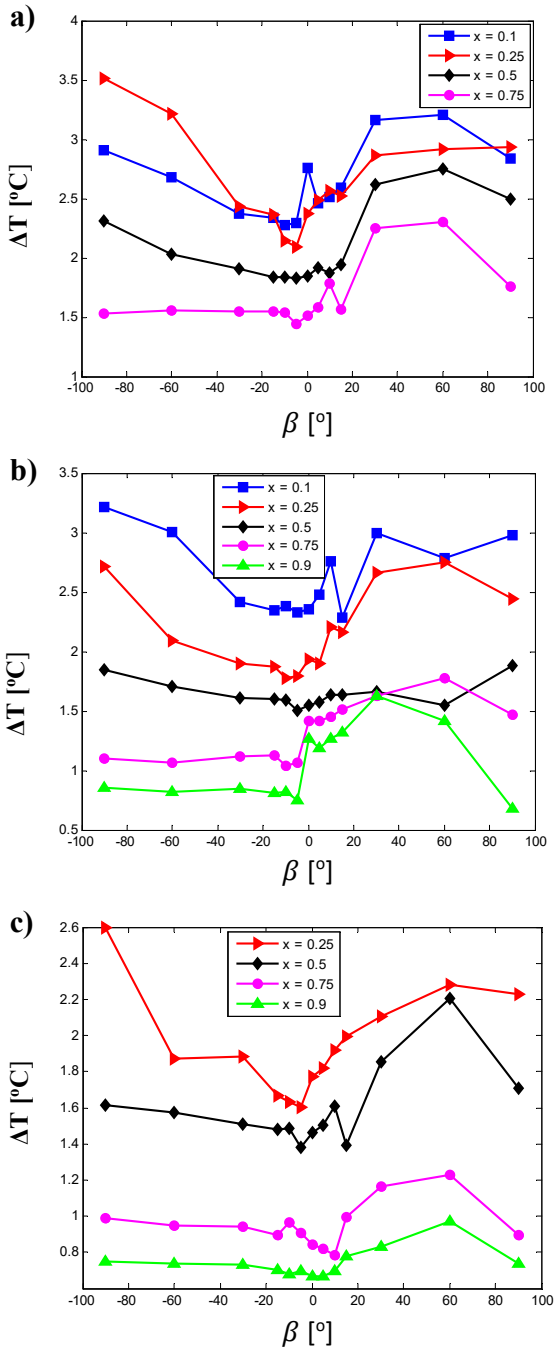

Fig. 3. The effects of mean vapour quality and inclination on the temperature difference (ΔT) for a mass velocity of: a) 200 kg/m^{2}s; b) 300 kg/m^{2}s; and c) 400 kg/m^{2}s.

less responsive to change in temperature. During this orientation, the fluid thickness reduces compared with the upward flow such that the thermal resistance and gravitational force are reduced, and shear force predominates. At low vapour qualities, the effect of gravitational force is significant hence the effect of inclination angle is noticeable. As the inclination angle increases during upward flows, the fluid thickness increases (increased thermal resistance) coupled with flow distribution that are more turbulent. Inclination has a significant impact on the temperature difference and generally decreases with quality, except for the low quality at a mass velocity of 200 $kgm^{-2}s^{-1}$. The temperature difference decreases or increases slightly between an inclination angle of -90^o and -15^o, after which it becomes unpredictable. Between +15^o and +90^o, there is an increase, which decreases after climaxing at an inclination angle of 60^o or 30^o.

Since the heat transfer coefficient and frictional pressure drop are the main contributors to the total entropy generation, it can be inferred that inclination angle and flow pattern have a considerable effect on entropy generation. Figs. 4 to 6 indicate the effects of inclination angle and quality on entropy generation rates ascribed to heat transfer, frictional pressure drop, total entropy generation rate, and Bejan number for a mass velocity of 200 $kgm^{-2}s^{-1}$ (Fig. 4), 300 $kgm^{-2}s^{-1}$ (Fig. 5) and 400 $kgm^{-2}s^{-1}$ (Fig. 6). Eq. (3) shows the direct influence of temperature difference and frictional pressure drop on entropy production as the results reveal that entropy generation attributable to heat transfer follows a similar pattern as temperature difference. The effect of inclination angle on entropy generation rate ascribed to frictional pressure drop decreases with mass velocity. During the downward flow, there is a slight increase in the velocity of the liquid assisted by gravitational pull, which leads to an increase in the shear force; hence the frictional pressure drop and entropy change due to it. Increased quality and mass velocity have an increasing effect on frictional pressure drop contribution to entropy generation. On the total entropy generation, at a low mass velocity (G = 200 $kgm^{-2}s^{-1}$), the effect of heat transfer dominates, and with an increase in the frictional contribution, both convective heat transfer and frictional pressure drop significantly influence it at a mass velocity of 300 $kgm^{-2}s^{-1}$. For a mass velocity of 400 $kgm^{-2}s^{-1}$, the frictional pressure drop dominates the total entropy generation rate. For the Bejan number, the effect of inclination also decreased with mass velocity. The Bejan number generally seems to increase with the inclination angle, especially between -60^o and +60^o. However, an increase in mass velocity and quality decreases the Bejan number.

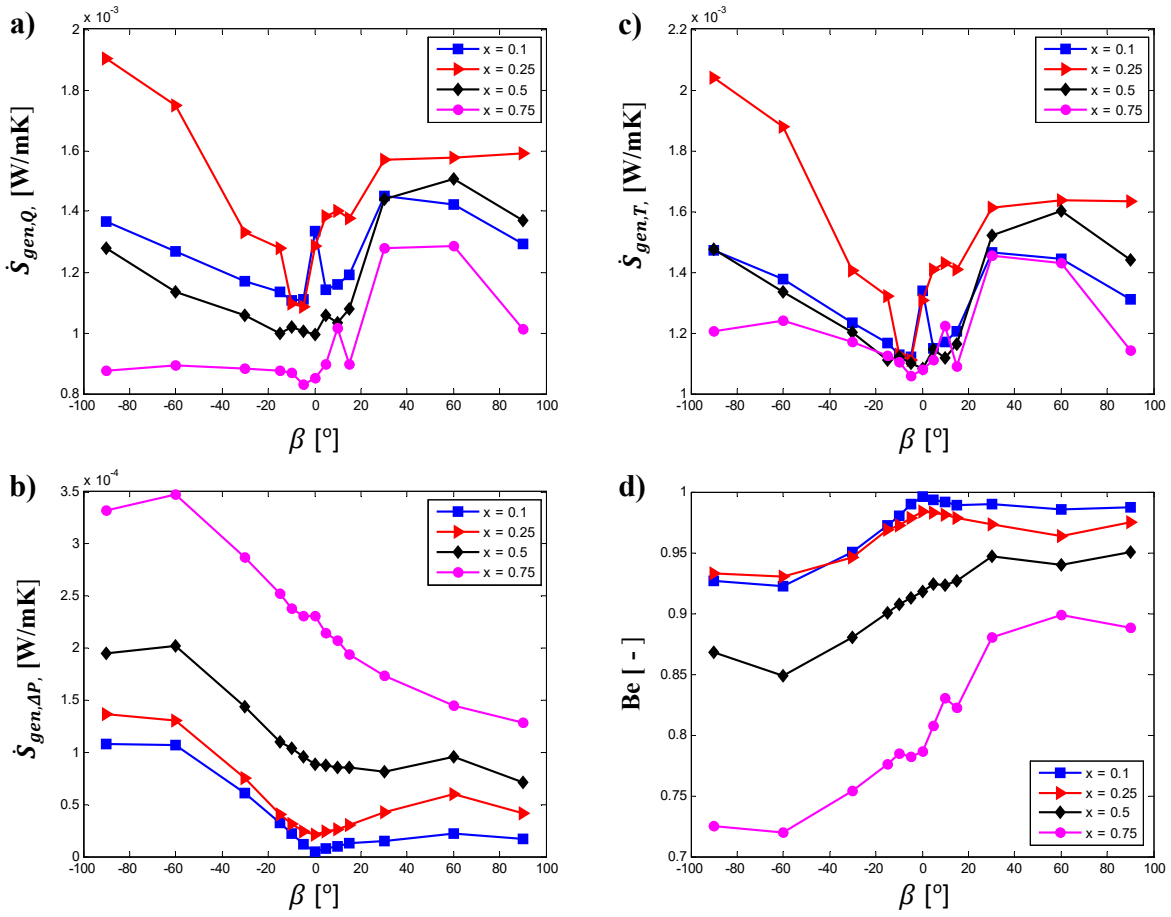

Fig. 4. The entropy generation versus inclination angle for: a) convective heat transfer; b) frictional pressure drop; c) total – addition of heat transfer and frictional pressure; and d) Bejan number for the mass velocity of 200 kg/m^{2}s.

Fig. 4a shows that entropy generation due to convective heat transfer and total entropy generation is at its maximum during vertically downward flow (β = -90°) at a vapour quality of 25%, but is at its minimum when the inclination angle is -5° at a vapour quality of 75%. There is a general decrease in entropy during the downward flow with an increase in inclination angle, except at a vapour quality of 75%, where the effect of the inclination angle seems insignificant. Fig. 4b shows an increase in entropy generation attributable to frictional pressure drop as the flow is inclined downwards. The maximum entropy generation is obtained at the inclination angle of -60° for vapour qualities of 50–75%, and -90° for vapour qualities of 10–25%. The minimum value occurs at the horizontal tube orientation for a vapour quality of 10%. The minimum Bejan value corresponds to an inclination angle of -60° and vapour quality of 75%, while the maximum value occurs during horizontal flow at 10% vapour quality.

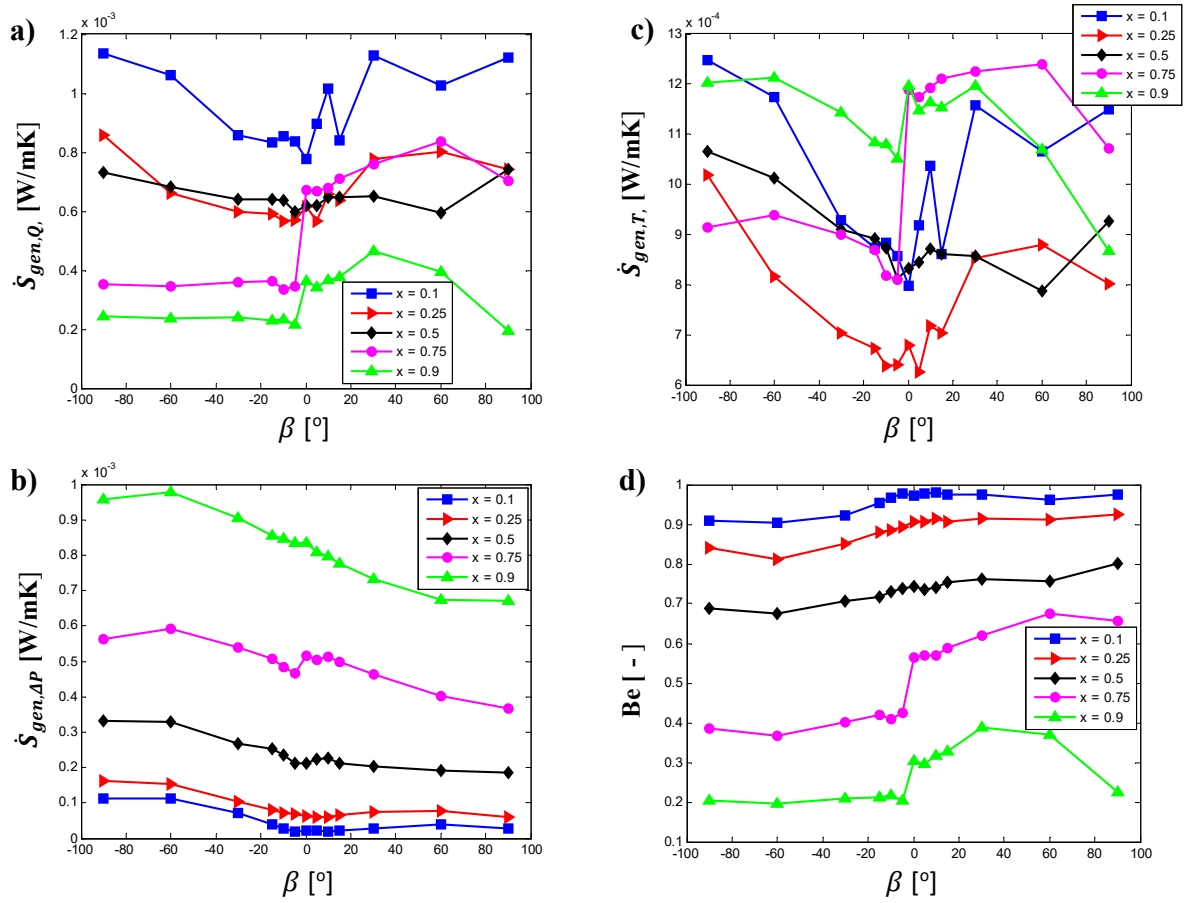

Fig. 5. The entropy generation versus inclination angle due to: a) convective heat transfer; b) frictional pressure drop; c) total – addition of heat transfer and frictional pressure; and d) Bejan number for the mass velocity of 300 kg/m^{2}s.

Fig. 5 shows that for a mass velocity of 300 kgm^{-2}s^{-1}, the profile of the convective heat transfer contribution to total entropy generation differs significantly from that of the total entropy generation rate, unlike the results obtained in Figs. 4a and 4c. This can be attributed to the increase in the frictional contribution. While the maximum values of both occur at the inclination of -90º, the minimum occurs at the inclination of +90ºand vapour quality of 90% for the heat transfer contribution and at +5º inclination and vapour quality of 25% for the total entropy generation rate. The maximum frictional pressure drop occurs at an inclination of -60º and vapour quality of 90%. The minimum corresponds to an inclination angle of -5º and vapour quality of 10%. In terms of the Bejan number, the maximum number is recorded at an inclination of +10º and a vapour quality of 10%, but the minimum number is recorded at -60º and vapour quality of 90%.

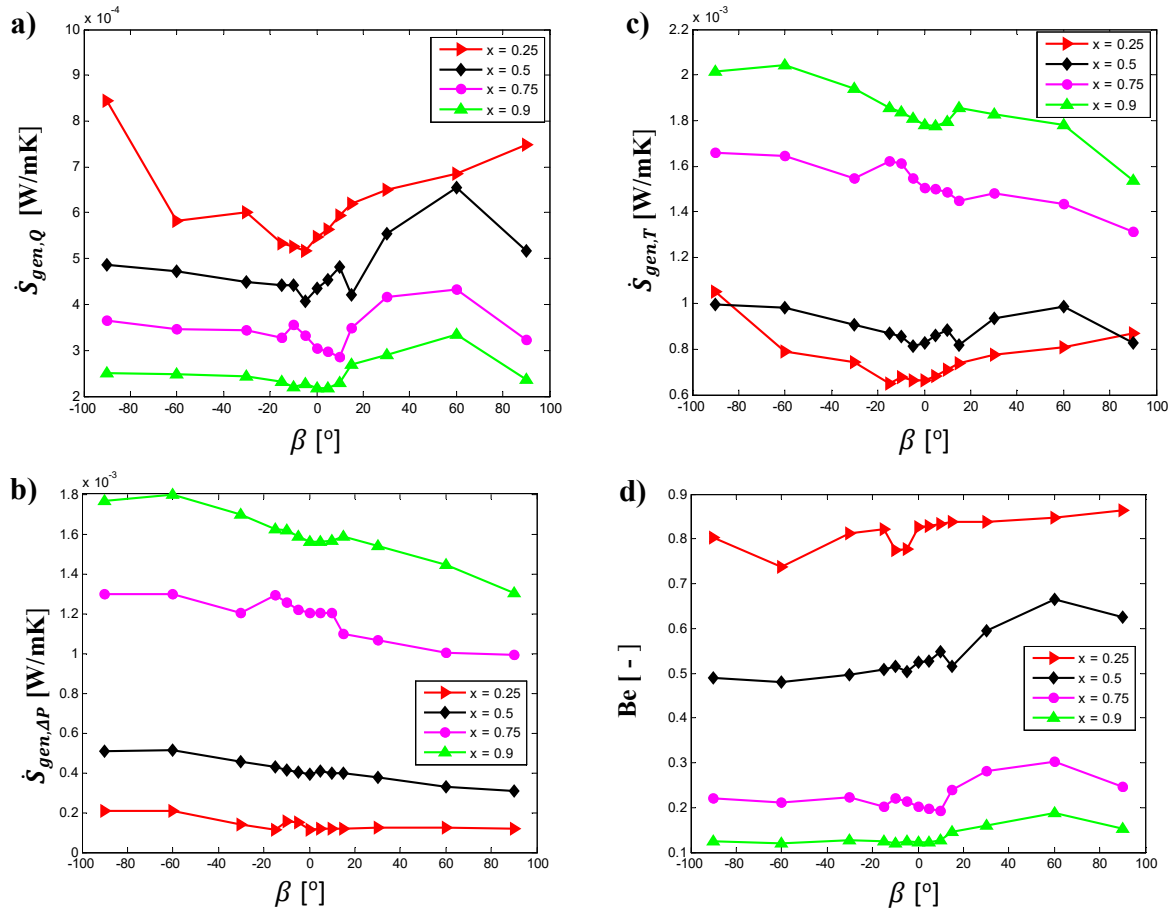

Fig. 6. The entropy generation versus inclination angle due to: a) convective heat transfer; b) frictional pressure drop; c) total – addition of heat transfer and frictional pressure; and d) Bejan number for the mass velocity of 400 kg/m^{2}s.

Fig. 6 reveals that, for a mass velocity of 400 kgm^{-2}s^{-1}, the frictional pressure drop is the controlling factor in the total entropy generation rate. As in Fig. 4b, frictional pressure drop entropy generation increases with vapour quality. The maximum and minimum heat transfer contributions to the entropy generation rate are at an inclination angle of -90° for a vapour quality of 25% and horizontal for a vapour quality of 90%, respectively. The total entropy generation rate has maximum and minimum values at an inclination of -60° for a vapour quality of 90% and at the inclination of -15° for a vapour quality of 25% (Fig. 6c).The Bejan number seems to be slightly affected by inclination angle for high qualities (x_m = 50–90%) between inclinations of -90° and 0°.

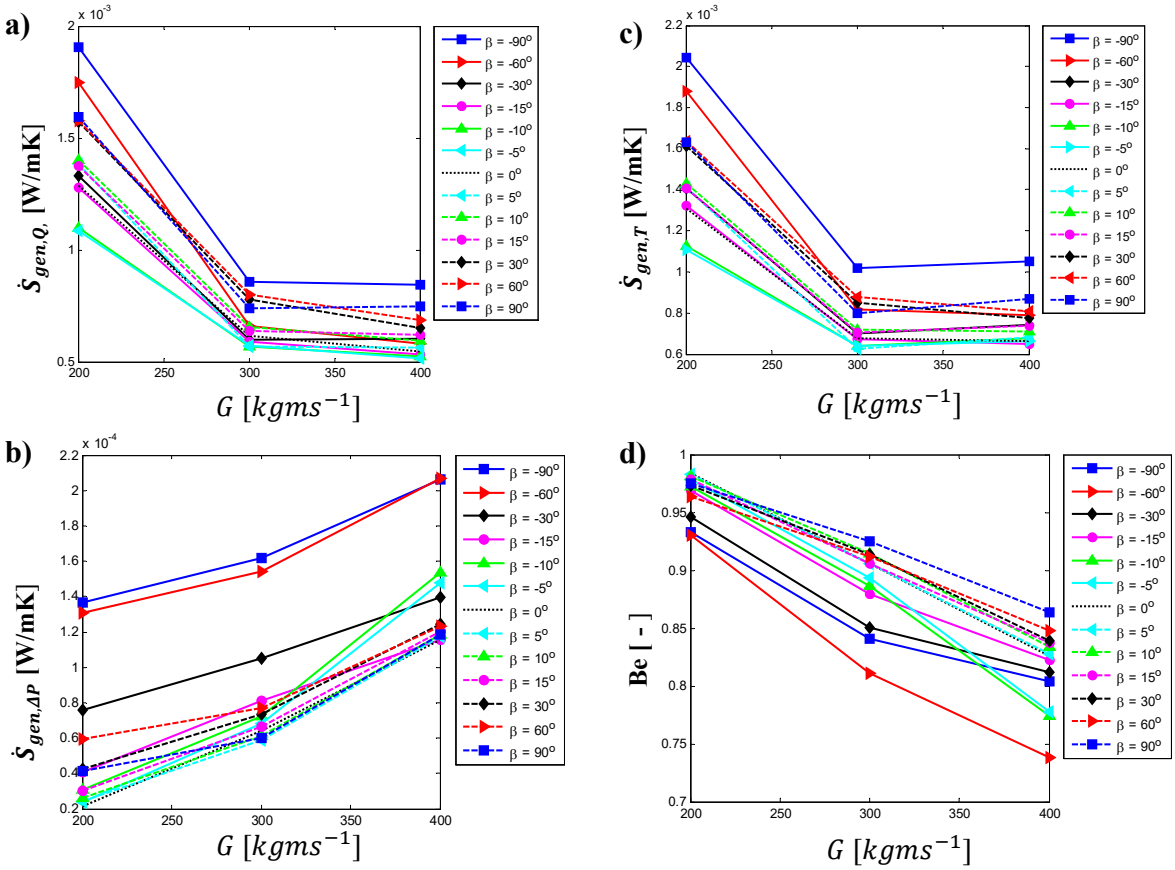

Fig. 7. The entropy generation versus mass velocity for different inclination angles due to: a) convective heat transfer; b) frictional pressure drop; c) total – addition of heat transfer and frictional pressure; and d) Bejan number for the quality of 25%.

The influences of mass velocity and inclination angle on entropy generation rates and the Bejan number for qualities of 25–75% are presented in Figs. 7 to 9. Increasing mass velocity (increased shear force) decreases temperature difference and entropy generation due to convective heat transfer, while the pressure drop and its contribution to total entropy generation increase. Fig. 7 shows the effect of mass velocity and inclination on the contributions of convective heat transfer and frictional pressure drop to and the total entropy generation rate and Bejan number for the vapour quality of 25%. The vertically downward flow shows a consistently higher thermal, frictional and total entropy generation rate, while inclinations of -5° and -10° give a minimum thermal contribution and total entropy generation. The high irreversibility (entropy generation rate) during the vertically downward flow may be attributed to the flow instabilities from Taylor

bubbles. The downward flows give a high frictional pressure drop, but the minimum exists during the horizontal and vertically upward flow. The lowest Bejan number is at an inclination of-60°, while the maximum values are at inclinations of +90° and +5°.

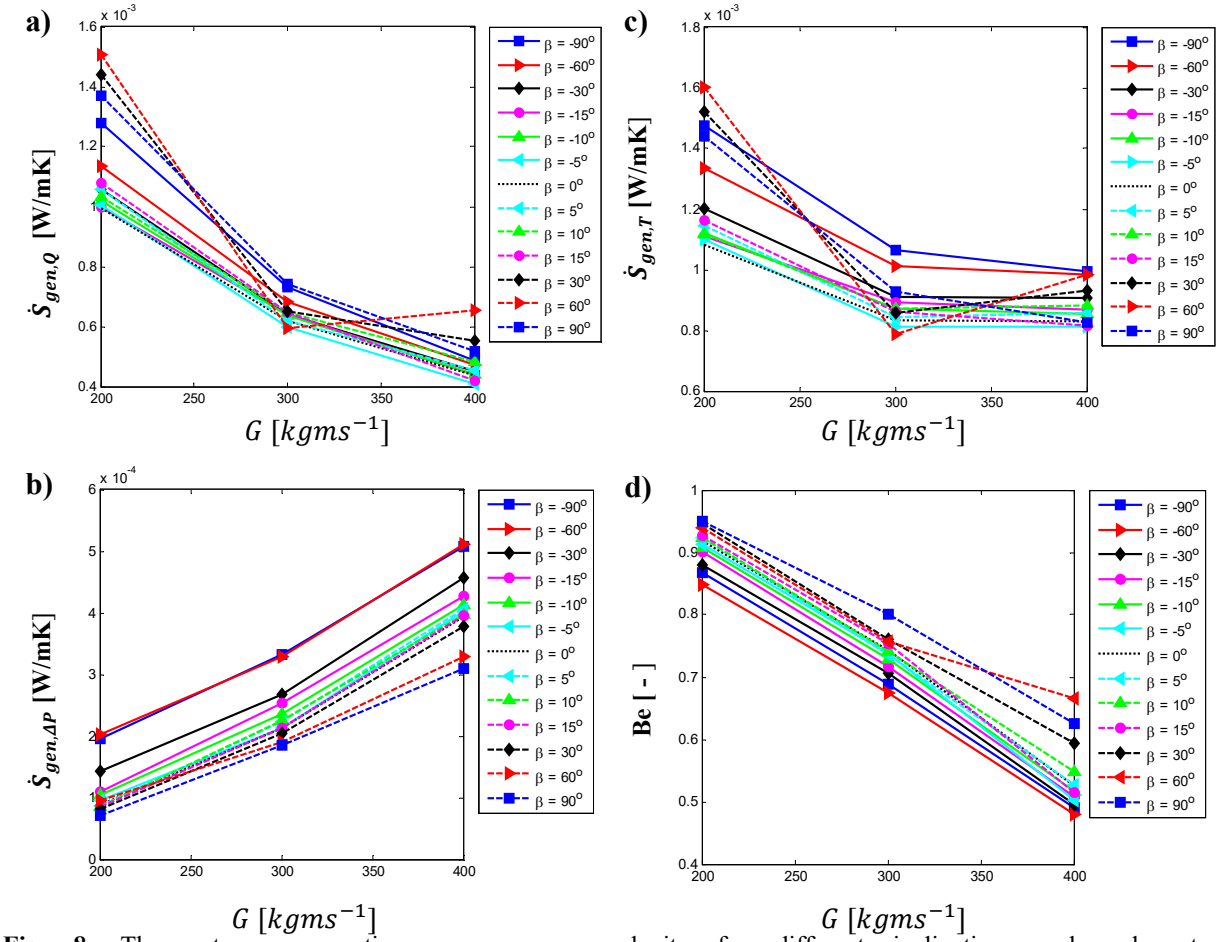

Fig. 8. The entropy generation versus mass velocity for different inclination angles due to: a) convective heat transfer; b) frictional pressure drop; c) total – addition of heat transfer and frictional pressure; and d) Bejan number for the quality of 50%.

With an increase in vapour quality to 50%, in Fig. 8, irreversibility in heat transfer contribution to the total entropy generation shifts to the upward flow as the maximum values now occur during upward flow (+60° and +90° inclinations). More flows during upward inclinations now possess high entropy generation. Total entropy generation now occurs during upward flow for mass velocities of 200 and 400 $kgm^{-2}s^{-1}$. The increase in pressure drop contribution during downward flow is still sufficient to maintain high total entropy generation during downward flow for the mass velocities of 300–400 $kgm^{-2}s^{-1}$. The low frictional pressure entropy generation

remains lower for upward flows than it does for downward flows. The Bejan numbers are higher during upward flows than during downward flows because of the low frictional contribution. The minimum consistently corresponds to -60°.

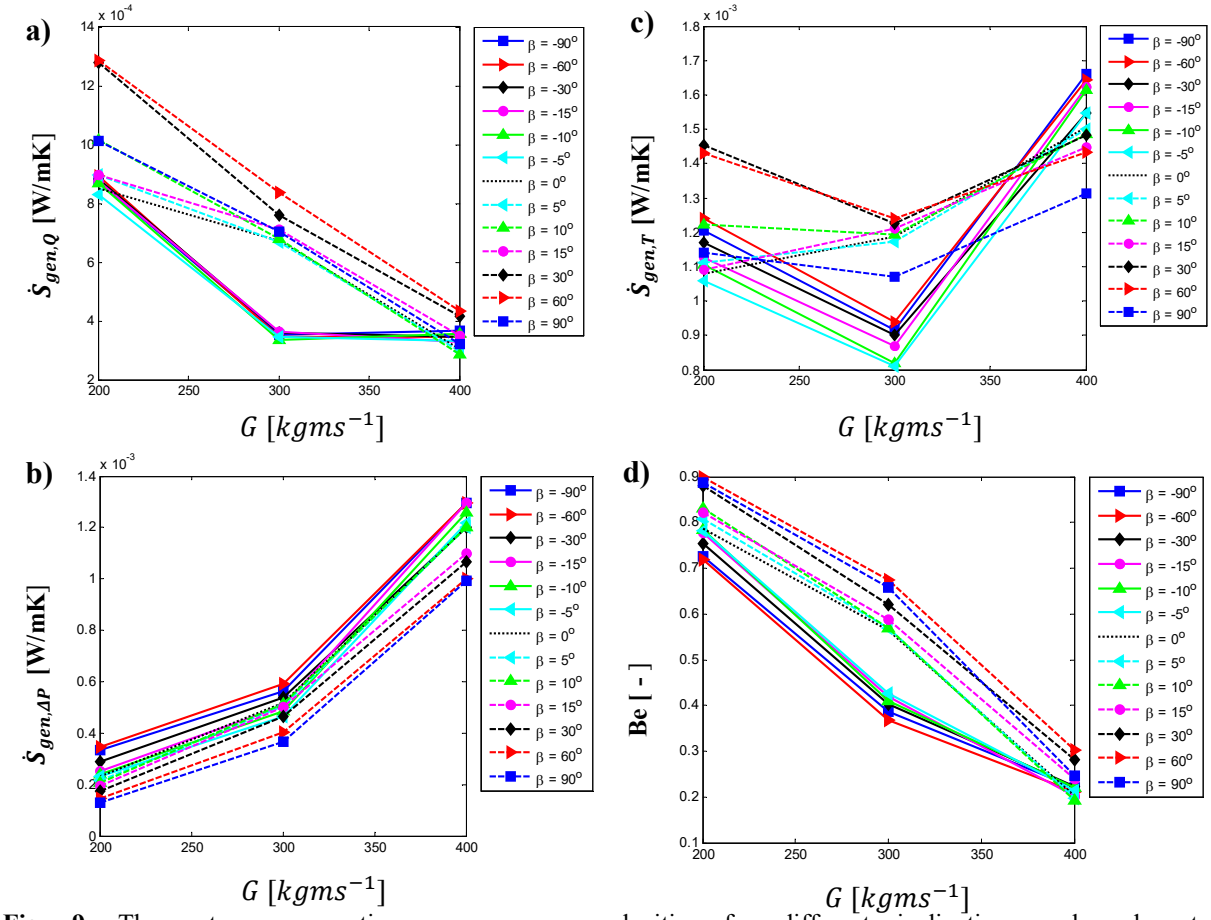

Fig. 9. The entropy generation versus mass velocities for different inclination angles due to: a) convective heat transfer; b) frictional pressure drop; c) total – addition of heat transfer and frictional pressure; and d) Bejan number for the quality of 75%.

Fig. 9 depicts the impacts of mass velocity and inclination on the convective heat transfer and pressure drop contributions to and total entropy generation and Bejan number for a vapour quality of 75%. The result shows that, at a high quality, the upward flows possess higher entropy generation rates than the downward. Only at a mass velocity of 400 $kgm^{-2}s^{-1}$ did more downward flow possess comparable entropy values, although these are still less than those obtainable at inclinations of+30° and +60°. In Fig. 9b, the downward flows still maintain higher frictional entropy generation rates when compared with the upward flows. Although the upward flows

possess higher total entropy generation for mass velocities of 200 and 300 $kgm^{-2}s^{-1}$, more downward flows possess high entropy for the mass velocity of 200 $kgm^{-2}s^{-1}$ (Fig. 9c). At a mass velocity of 400 $kgm^{-2}s^{-1}$, the downward flows exhibit more irreversibility, basically due to frictional pressure drop. In Fig. 9d, a higher Bejan number is obtained during upward flows than during downward flows.

An increase in the vapour quality (decreased thermal resistance) results in a decreased temperature difference and, consequently, the entropy due to convective heat transfer. On the other hand, the shear force increased, resulting in a more significant frictional pressure difference and its contribution to the total entropy generation. Figs. 10–12 present the effects of quality and inclination angle on entropy generation rates attributable to heat transfer, pressure drop, total entropy generation rate, and Bejan number for the mass velocities of 200–400 $kgm^{-2}s^{-1}$. The frictional contribution to the total entropy generation monotonically increases with quality, but the Bejan number displays the reverse.

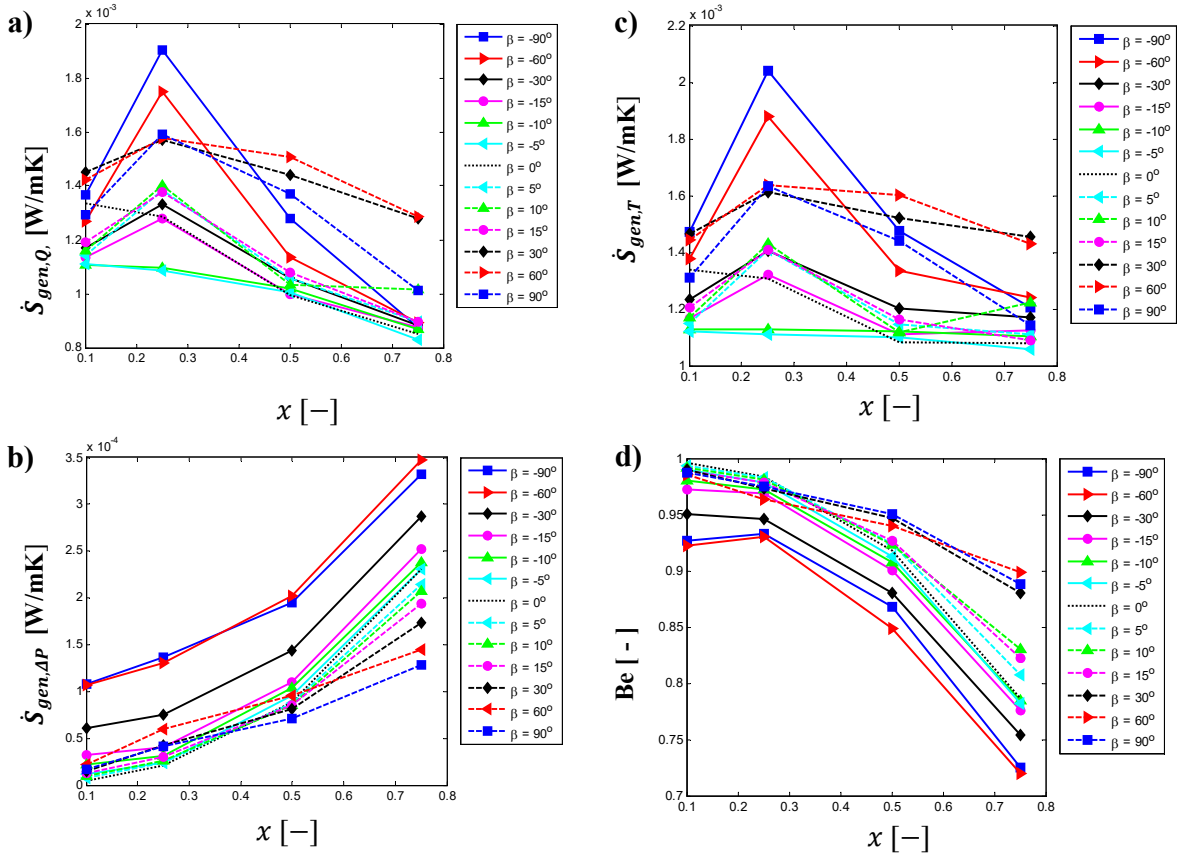

Fig. 10. The entropy generation versus mass velocities for different inclination angles due to: a) convective heat transfer; b) frictional pressure drop; c) total – addition of heat transfer and frictional pressure; and d) Bejan number for the mass velocity of 200 kg/m^2s.

Fig.10 illustrates the influences of quality and inclination angle on the heat transfer and frictional pressure drop contributions to the total entropy generation rate, total entropy generation rate, and Bejan number for a mass velocity of 200 $kgm^{-2}s^{-1}$. Results reveal that, except for a vapour quality of 25%, where high entropy generation occurs during downward flow due to flow pattern transitioning between stratified-wavy and intermittent, and churn at an inclination of -60^o and -90^o, the upward flows possess higher entropy generation. For this mass velocity, the overall minimum occurs for an inclination angle of -5^o and vapour quality of 75%. The downward flows exhibit higher frictional entropy generation rates, while the horizontal and vertical upward flows give the minimum. The total entropy generation offers a similar profile as the convective heat transfer contribution because of the predominance of the convective heat transfer contribution compared with the frictional pressure drop. The difference in the pattern is a result of the frictional pressure drop that increases with quality. Fig. 10d indicates that the Bejan numbers are lower for downward flows with a maximum during the horizontal flow at the quality of 10% and a minimum during downward flow (-60^o inclination) for a quality of 75%.

Fig. 11 reveals the effects of mean vapour quality and inclination angle on the convective heat transfer and frictional pressure drop contributions to and the total entropy generation rate and Bejan number for a mass velocity of 300 $kgm^{-2}s^{-1}$. The result shows that, for mean vapour qualities of 10–50%, the convective heat transfer entropy generation rates for upward and downward flows are comparable. However, for larger qualities, upward flows have significantly higher values than downward flows. The maximum corresponds to an inclination of ± 90^o (x_m = 10%), while the minimum is at an inclination of +90^o (x_m = 90%). The downward flows continue to have predominantly higher frictional entropy generation rates (Fig. 11b). Due to the impact of frictional pressure drop, qualities of 10–50% have higher entropy generation for an inclination of -90^o, and downward flows are comparable with upward flows at 90% quality. The Bejan number is higher for upward flows than for downward flows.

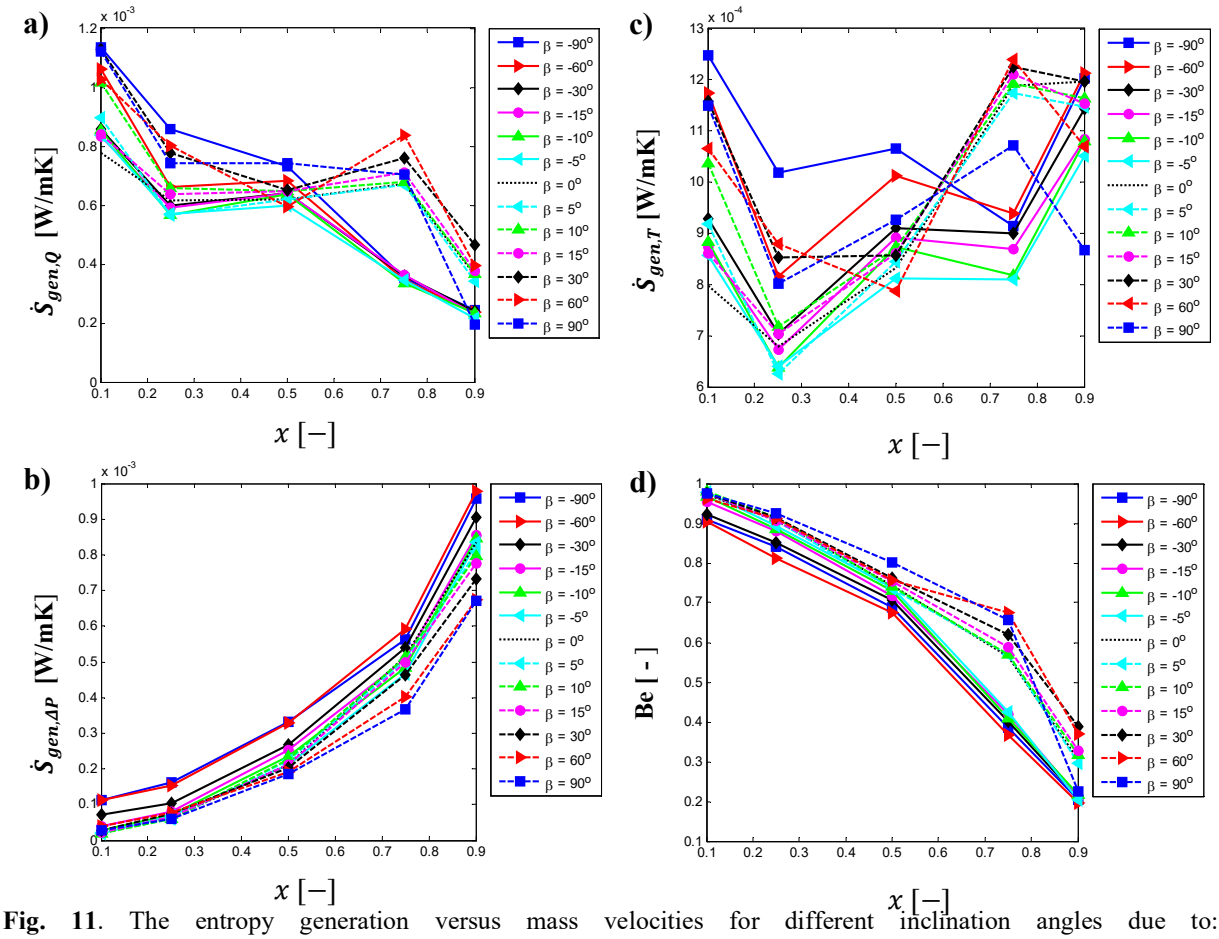

Fig. 11. The entropy generation versus mass velocities for different inclination angles due to: a) convective heat transfer; b) frictional pressure drop; c) total – addition of heat transfer and frictional pressure; and d) Bejan number for the mass velocity of 300 kg/m^{2}s.

Fig. 12 illustrates the variation of entropy generation rate due to convective heat transfer, frictional pressure drop, total entropy generation rate, and Bejan number for a mass velocity of 400 kgm^{-2}s^{-1}. The result (Fig. 12a) shows that upward flows, particularly for inclination angles of +30^o and +60^o, dominate the entropy generation rate due to heat transfer; however, downward flow with an inclination of -90^o has the highest value at the quality of 25%.The downward flow maintains the lead with regard to entropy generation attributable to friction (Fig. 12b). For the total entropy generation rate, at low qualities of 25–50%, apart from the vertically downward flow that has relatively higher entropy generation, both upward and downward flows are comparable. However, for larger vapour qualities (75–90%), the downward flows give higher values than the upward flows (Fig. 12c) due to higher shear force. The upward flows present higher Bejan numbers compared to the downward flows (Fig. 12d).

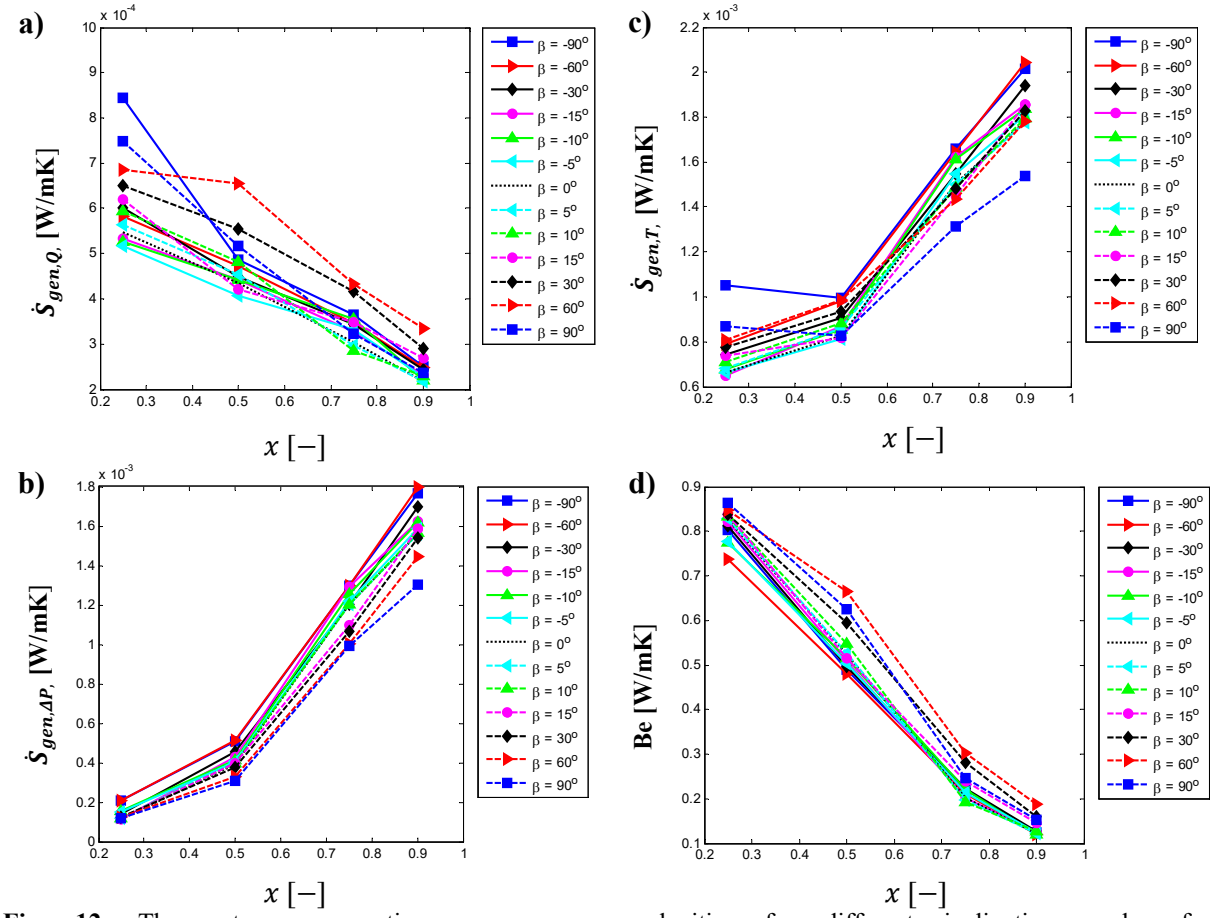

Fig. 12. The entropy generation versus mass velocities for different inclination angles for: a) convective heat transfer; b) frictional pressure drop; c) total – addition of heat transfer and frictional pressure; and d) Bejan number for the mass velocity of 400 kg/m^{2}s.

Fig. 13 shows the optimal inclination angles and mean vapour qualities for each of the mass velocities that give the minimal entropy generation. However, for the evaluation of the Bejan number, the optimum inclination angle coincides with the condition when the ratio of the entropy generation rate due to pressure drop to the entropy generation rate due to heat transfer approaches zero. The optimal inclination angles seem to occur between -10° and +90°. For the convective heat transfer contribution and the total entropy generation rates, the optimal angle mainly fall between -10° and +10°. For the frictional pressure drop contribution, the low mean vapor qualities (10-25%) produce an optimal inclination angle between -5° and +5°, while for mean quality of 50–90%, it exists at +90°. The Bejan number mostly has the optimal between +60° and +90°.

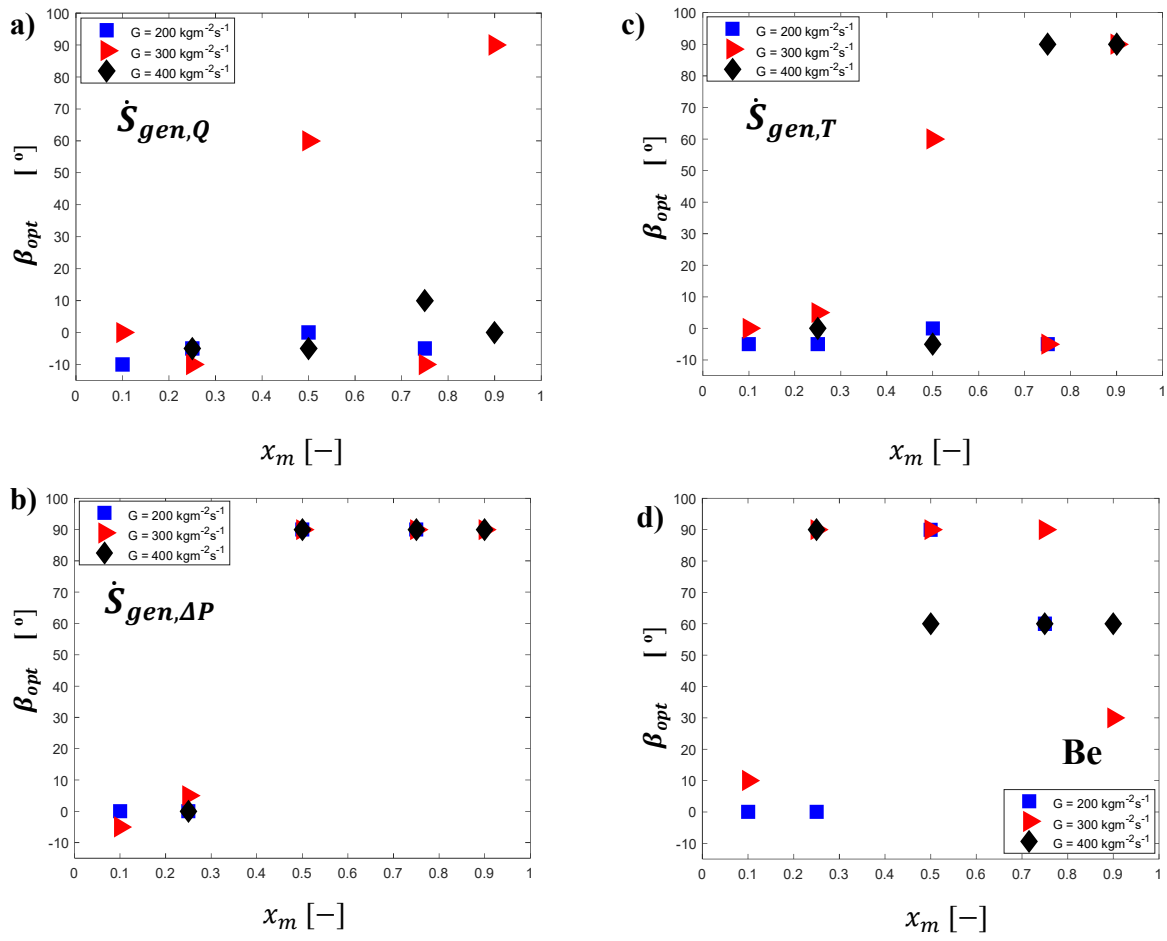

Fig. 13. The optimal inclination angle versus the mean vapour quality for different mass velocities for the: a) entropy generation rate attributable to convective heat transfer, b) entropy generation rate attributable to frictional pressure drop, c) total entropy generation rate and, d). Bejan number.

5.0 Conclusions

This study presents the effects of inclination angle, mass velocity, and quality on entropy generation rates attributable to heat transfer and frictional pressure drop, total entropy generation rate, and Bejan number during convective condensation in inclined microfinned tubes at a saturation temperature of 40 °C. The enhanced tube's outer diameter, heat transfer, and pressure drop lengths are 9.55 mm, 1.488 m, and 1.704 m, respectively. The mean vapour quality varies between 10 and 90%, mass velocity between 200 and 400 $kgm^{-2}s^{-1}$, and 13 inclination angles between vertically upward and downward flows.

(1). Results show that with an increase in the quality and mass velocity the entropy generation due to frictional pressure drop increases while that due to heat transfer decreases.

(2). At low mass velocity of 200 $kgm^{-2}s^{-1}$ the entropy generation due to heat transfer is more significant compared to that due to pressure drop and influences the response of the total entropy generation to inclination angle whereas at high mass velocity of 400 $kgm^{-2}s^{-1}$ the reverse is the case.

(3). An optimal inclination that corresponds to the minimum entropy generation for different mean vapour qualities and mass velocities is also obtained. This paper recommends that in the design and application of a microfinned condensing unit, the optimal inclination angle of $-10^{\circ} \leq \beta \leq +10^{\circ}$ is required to achieve minimal total entropy generation for vapour qualities equal to or less than 75%, (except for the cases of quality of 50% for mass velocity of 300 $kgm^{-2}s^{-1}$ ($\beta = +60^{\circ}$) and quality of 75% for mass velocity of 400 $kgm^{-2}s^{-1}$ ($\beta = +90^{\circ}$)), whereas it is $+90^{\circ}$ for qualities greater.

(4). The optimal inclination angle that gives the highest Bejan number corresponds to the condition when the ratio of the entropy generation rate due to pressure drop to that due to heat transfer approaches zero.

Acknowledgement

The funding support obtained from the CSIR, NRF, Stellenbosch University/University of Pretoria, TESP, SANERI/SANEDI, NAC, and EEDSM Hub is acknowledged and well appreciated.

References

Abu-Hamdeh, N. H., Bantan, R. A., and Alimoradi, A. (2020). Heat transfer optimization through new form of pin type of finned tube heat exchangers using the exergy and energy analysis. *International Journal of Refrigeration*.

Adelaja, A. O., Dirker, J., and Meyer, J. P. (2016). Convective condensation heat transfer of R134a in tubes at different inclination angles. *International Journal of Green Energy*, *13*(8), 812-821.

Adelaja, A. O., Dirker, J., and Meyer, J. P. (2017). Experimental study of the pressure drop during condensation in an inclined smooth tube at different saturation temperatures. *International Journal of Heat and Mass Transfer*, *105*, 237-251.

Adelaja, A. O., Dirker, J., and Meyer, J. P. (2019). Condensation Heat Transfer Coefficients and Enhancements of R134a in Smooth and Microfin Inclined Tubes. *Energy Procedia*, *158*, 5299-5304.

Adelaja, A. O., Ewim, D. R., Dirker, J., and Meyer, J. P. (2019). Heat transfer, void fraction and pressure drop during condensation inside inclined smooth and microfin tubes. *Experimental Thermal and Fluid Science*, *109*, 109905.

Adelaja, A.O., Ewim, D.R.E., Dirker, J., Meyer, J.P. (2020). An improved heat transfer correlation for condensation inside inclined smooth tubes. *International Communications in Heat and Mass Transfer*, 117, 104746.

Adeyinka, O., and Naterer, G. (2004). Optimization correlation for entropy production and energy availability in film condensation. *International Communications in Heat and Mass Transfer*, *31*(4), 513-524.

Ahmad, S. N., Priyadarshi, N., Bhoi, A. K., Kumar, M., and Sharma, A. (2018). Exergy analysis of double tube heat exchanger for parallel flow arrangement. IOP Conference Series: Materials Science and Engineering,

Bejan, A. (1977). The concept of irreversibility in heat exchanger design: counterflow heat exchangers for gas-to-gas applications.

Bejan, A. (1978). General criterion for rating heat-exchanger performance. *International Journal of Heat and Mass Transfer*, *21*(5), 655-658.

Bejan, A. (1979). A study of entropy generation in fundamental convective heat transfer.

Bejan, A. (1980). Second law analysis in heat transfer. *Energy*, *5*(8-9), 720-732.

Bejan, A. (1996). Entropy generation minimization: The new thermodynamics of finite‐size devices and finite‐time processes. *Journal of Applied Physics*, *79*(3), 1191-1218.

Bejan, A. (2000). Entropy generation minimization: The method and its applications. ICHMT DIGITAL LIBRARY ONLINE,

Bejan, A., Tsatsaronis, G., and Moran, M. J. (1995). *Thermal design and optimization*. John Wiley & Sons.

Bhagwat, S. M., and Ghajar, A. J. (2014). A flow pattern independent drift flow model based void fraction correlation for a wide range of gas-liquid two-phase flow. *International Journal of Multiphase Flow*, *59*, 188-205.

Cavallini, A. (2002). Heat transfer and energy efficiency of working fluids in mechanical refrigeration. *Bulletin of the International Institute of Refrigeration*, *2002*(6), 4-21.

Chen, B. C., Wu, J. R., and Yang, S. A. (2008). Entropy generation of forced convection film condensation from downward flowing vapors onto a horizontal tube. *Journal of the Chinese Institute of Engineers*, *31*(2), 349-354.

Chen, X., Zhao, T., Zhang, M.-Q., and Chen, Q. (2019). Entropy and entransy in convective heat transfer optimization: A review and perspective. *International Journal of Heat and Mass Transfer*, *137*, 1191-1220.

Ewim, D., Meyer, J. P., and Abadi, S. N. R. (2018). Condensation heat transfer coefficients in an inclined smooth tube at low mass fluxes. *International Journal of Heat and Mass Transfer*, *123*, 455-467.

Galovic, A., Virag, Z., and Zivic, M. (2003). Analytical entropy analysis of recuperative heat exchangers. *Entropy*, *5*(5), 482-495.

Gheorghian, A. T., Dobrovicescu, A., Popescu, L. G., Cruceru, M., & Diaconu, B. M. (2015). Entropy generation assessment criterion for compact heat transfer surfaces. *Applied Thermal Engineering*, *87*, 137-149.

Holagh, S. G., Abdous, M. A., Shamsaiee, M., and Saffari, H. (2020). Assessment of heat transfer enhancement technique in flow boiling conditions based on entropy generation analysis: twisted-tape tube. *Heat and Mass Transfer*, *56*(2), 429-443.

Imteyaz, B., and Zubair, S. M. (2018). Effect of pressure drop and longitudinal conduction on exergy destruction in a concentric-tube micro-fin tube heat exchanger. *International Journal of Exergy*, *25*(1), 75-91.

Kaiser, V. (1993). *Industrial energy management: refining petrochemicals and gas processing techniques*. Editions Technip.

Keklikcioglu, O., Dagdevir, T., and Ozceyhan, V. (2020). Second law analysis of a mixture of ethylene glycol/water flow in modified heat exchanger tube by passive heat transfer enhancement technique. *Journal of Thermal Analysis and Calorimetry*, 1-14.

Khaboshan, H. N., and Nazif, H. R. (2019). Entropy generation analysis of convective turbulent flow in alternating elliptical axis tubes with different angles between pitches; a numerical investigation. *Heat and Mass Transfer*, *55*(10), 2857-2872.

Kumar, C. N., and Ilangkumaran, M. (2019). Experimental study on thermal performance and exergy analysis in an internally grooved tube integrated with triangular cut twisted tapes consisting of alternate wings. *Heat and Mass Transfer*, *55*(4), 1007-1021.

Li, G. C., and Yang, S. A. (2006). Thermodynamic analysis of free convection film condensation on an elliptical cylinder. *Journal of the Chinese Institute of Engineers*, *29*(5), 903-908.

Lin, W., Lee, D., and Peng, X. (2001). Condensation performance in horizontal tubes with second‐law consideration. *International journal of energy research*, *25*(11), 1005-1018.

McClintock, F. (1951). The design of heat exchangers for minimum irreversibility. *ASME paper*, *51*.

Meyer, J. P., Dirker, J., and Adelaja, A. O. (2014). Condensation heat transfer in smooth inclined tubes for R134a at different saturation temperatures. *International Journal of Heat and Mass Transfer*, *70*, 515-525.

Meyer, J. P., and Ewim, D. (2018). Heat transfer coefficients during the condensation of low mass fluxes in smooth horizontal tubes. *International Journal of Multiphase Flow*, *99*, 485-499.

Ranasinghe, J., and Reistad, G. (1990). 'Irreversibility in Heat Exchanger-Design and Optimization. *Compact Heat Exchangers*, 365.

Ratts, E. B., and Raut, A. G. (2004). Entropy generation minimization of fully developed internal flow with constant heat flux. *J. Heat Transfer*, *126*(4), 656-659.

Revellin, R., Lips, S., Khandekar, S., and Bonjour, J. (2009). Local entropy generation for saturated two-phase flow. *Energy*, *34*(9), 1113-1121.

Saechan, P., and Wongwises, S. (2008). Optimal configuration of cross flow plate finned tube condenser based on the second law of thermodynamics. *International Journal of Thermal Sciences*, *47*(11), 1473-1481.

Sahiti, N., Krasniqi, F., Fejzullahu, X., Bunjaku, J., and Muriqi, A. (2008). Entropy generation minimization of a double-pipe pin fin heat exchanger. *Applied Thermal Engineering*, *28*(17-18), 2337-2344.

Saouli, S., and Aïboud-Saouli, S. (2004). Second law analysis of laminar falling liquid film along an inclined heated plate. *International Communications in Heat and Mass Transfer*, *31*(6), 879-886.

See, Y., and Leong, K. (2020). Entropy generation for flow boiling on a single semi-circular minichannel. *International Journal of Heat and Mass Transfer*, *154*, 119689.

Wang, W., Zhang, Y., Liu, J., Wu, Z., Li, B., and Sundén, B. (2018). Entropy generation analysis of fully-developed turbulent heat transfer flow in inward helically corrugated tubes. *Numerical Heat Transfer, Part A: Applications*, *73*(11), 788-805.

Wang, Y., and Huai, X. (2018). Heat transfer and entropy generation analysis of an intermediate

heat exchanger in ads. *Journal of Thermal Science*, *27*(2), 175-183.

Yang, S.-A., Li, G.-C., and Yang, W.-J. (2007). Thermodynamic optimization of free convection film condensation on a horizontal elliptical tube with variable wall temperature. *International Journal of Heat and Mass Transfer*, *50*(23-24), 4607-4613.

Zhang , H., Jiangfeng, G., Xiulan, H., and Xinying, C. (2019). Thermodynamic performance analysis of supercritical pressure CO2 in tubes. *International Journal of Thermal Sciences*, *146*.

Zhao, X., Jiaqiang, E., Zhang, Z., Chen, J., Liao, G., Zhang, F., Leng, E., Han, D., and Hu, W. (2020). A review on heat enhancement in thermal energy conversion and management using Field Synergy Principle. *Applied Energy*, *257*, 113995.